

International Journal of Hydrogen Energy

Effect of Alkaline Fuel Cell Catalyst on Deuterium Isotope Separation

--Manuscript Draft--

Manuscript Number:	HE-D-20-03029R2
Article Type:	Full Length Article
Section/Category:	Fuel Cells & Applications
Keywords:	Deuterium; Separation factor; Ruthenium; Fuel Cell; Hydrogen isotopes
Corresponding Author:	Hisayoshi Matsushima, PhD Hokkaido University Sapporo, JAPAN
First Author:	Risako Tanii
Order of Authors:	Risako Tanii
	Ryota Ogawa
	Hisayoshi Matsushima, PhD
	Mikito Ueda
	Richard Dawson
Abstract:	<p>Fuel cells (FC) have been developed for automobiles and stationary power units. In addition to a power generator function, we propose a new application of hydrogen isotope separation. In this paper, deuterium (D) separation is investigated by two types of AFCs with platinum (Pt) or ruthenium (Ru) anode catalysts. The characteristics of the AFCs are evaluated by pure protium (H) or deuterium gas separately. In the case of Pt catalyst, the cell current/voltage curves show similar results for both gases. But a remarkable decrease in the voltage value is observed probably due to the mass transportation (diffusion) limitation at Ru catalyst. The limitation effect was larger for D₂ than H₂ gas. The AC impedance measurements supports that the slow reaction rate of D₂ gas on Ru catalyst. The separation experiments are verified with hydrogen gas mixed with 1 at% D. The D is diluted in the unreacted gas discharged from AFC with Pt catalyst, but it is concentrated with Ru one. The inverse response may be attributed to the elementary process of the hydrogen oxidation reaction and the difference in the adsorption energy of gas and water molecules on the catalyst surface.</p>

November 11, 2020

Prof. Renju Zacharia
Assistant Subject Editor
International Journal of Hydrogen Energy

Dear Prof. Renju Zacharia

Re: HE-D-20-03029

Authors: R. Tanii, R. Ogawa, H. Matsushima, M. Ueda and R. Dawson

Title: "Effect of Alkaline Fuel Cell Catalyst on Deuterium Isotope Separation"

Thank you for your letter of Nov. 11, 2020 and for the reviewer's comments concerning our manuscript. We have modified reference format. The changed parts are marked by Yellow color.

We hope that the revised manuscript is now suitable for publication.

Thank you very much for your kind considerations in advance.

Yours sincerely,

Dr. Hisayoshi Matsushima
Graduate School of Engineering
Hokkaido University
Kita-Ku, Sapporo 060-8628, Japan
Tel&Fax: +81-11-706-6352
E-mail: matsushima@eng.hokudai.ac.jp

Answer to Reviewer 3

Thank you for your comments.

1. Formatting the references in the style of Int. J. Hydrog. Energy (Including the reference title).

We corrected the reference format.

2. Adding further and newer references (preferably from IJHE).

Some references are added.

[35] M. Y. Yang, J. B. Zhou, L. P. Gao, The purification of hydrogen isotopes expelled from nuclear fusion reactors by a combined process, Int. J. Hydrog. Energy 2020;45: 13596-13600.

[36] W. J. Byeon, S. K. Lee, S. J. Noh, Transport of hydrogen and deuterium in 316LN stainless steel over a wide temperature range for nuclear hydrogen and nuclear fusion applications, Int. J. Hydrog. Energy 2020;45: 8827-8832.

[37] M. Glugla, R. Lasser, L. Dorr, D. K. Murdoch, R. Haange, H. Yoshida, The inner deuterium/tritium fuel cycle of ITER, Fusion Eng. Des. 2003;69:39-43.

Highlights

- Deuterium isotope separation was conducted by alkaline fuel cell.
- The separation mechanism was reversed between Ru and Pt anode catalysts.
- The reason might be attributed to the elementary reaction of HOR and the adsorption energy of hydrogen atoms on the catalysts.

Effect of Alkaline Fuel Cell Catalyst on Deuterium Isotope Separation

Risako Tanii^{1z}, Ryota Ogawa¹, Hisayoshi Matsushima^{1*}, Mikito Ueda¹ and Richard Dawson²

¹Faculty of Engineering, Hokkaido University,

Kita 13 Nishi 8, Sapporo, Hokkaido 060-8628, Japan.

**Corresponding Author: matsushima@eng.hokudai.ac.jp*

Tel. & Fax +81-11-7066352

² Faculty of Engineering, Lancaster University,

Gillow Avenue, Lancaster LA1 4YW, UK.

^zNew Address; Toyota Motor Corporation,

Toyota-cho, Toyota, Aichi 471-8571, Japan.

Abstract

Fuel cells (FC) have been developed for automobiles and stationary power units. In addition to a power generator function, we propose a new application of hydrogen isotope separation. In this paper, deuterium (D) separation is investigated by two types of AFCs with platinum (Pt) or ruthenium (Ru) anode catalysts. The characteristics of the AFCs are evaluated by pure protium (H) or deuterium gas separately. In the case of Pt catalyst, the cell current/voltage curves show similar results for both gases. But a remarkable decrease in the voltage value is observed probably due to the mass transportation (diffusion) limitation at Ru catalyst. The limitation effect was larger for D₂ than H₂ gas. The AC impedance measurements supports that the slow reaction rate of D₂ gas on Ru catalyst. The separation experiments are verified with hydrogen gas mixed with 1 at% D. The D is diluted in the unreacted gas

discharged from AFC with Pt catalyst, but it is concentrated with Ru one. The inverse response may be attributed to the elementary process of the hydrogen oxidation reaction and the difference in the adsorption energy of gas and water molecules on the catalyst surface.

Keywords: Deuterium; Separation factor; Ruthenium; Fuel Cell; Hydrogen isotopes

1. Introduction

Hydrogen as an energy vector is very important for addressing world energy and environmental issues. Green hydrogen, in which carbon dioxide is not involved, is produced by water electrolysis and can then be utilized by FCs, thus providing a route to clean energy storage. Hence, when the primary electrical generation is via renewables such as wind, the system can be considered 'green'. The hydrogen energy society will be established in the automobile industry as one of the first main commercial applications.

There are several types of FCs which are usually classified by their electrolyte type. Alkaline fuel cells (AFCs) were the first variant to be developed for commercial usage and were employed in space applications due to their high reliability [1, 2]. These alkaline fuel cells used a liquid electrolyte but more recently, FCs using anion exchange membranes have been developed [3]. Alkaline fuel cells have an advantage of less cathode overpotential than other FCs allowing cells to be run at higher efficiencies. This also has significant impacts on cost, because AFCs can use non-precious catalysts or low precious metal loadings and inexpensive KOH as an electrolyte [4, 5]. However, the slow kinetic of hydrogen oxidation reaction (HOR) is still a problem [6-8]. It is reported that Pt-Ru alloy catalysts improve HOR and overtake the performance of Pt [9, 10]. Therefore, it is worthwhile investing Ru catalyst for HOR particularly as it is one of the least expensive platinum group metals.

Fuel cells have been much researched and developed as power devices, while the hydrogen isotopes separation as a new application has been explored although to a much lesser extent [11-14]. There exist three hydrogen isotopes: protium (H), deuterium (D) and tritium (T). D is used as a neutron moderator in heavy water reactors. The D-T reaction is involved in energy production in fusion reactors, which are expected to represent the next generation of nuclear energy. Therefore, large amounts of these isotopes are required for the energy industry. However, the separation and purification are difficult because of the similarity in physical and chemical properties. Research on hydrogen isotope

separation began in the 1930s [15, 16]. Many researchers have studied a variety of the separation methods, including water distillation [17, 18], chemical exchange [19], water electrolysis [20-22], and the combined electrolysis catalytic exchange (CECE) [23]. Electrolysis is the most efficient way, but it still has the disadvantage of high electricity consumption.

To overcome this drawback, the authors previously proposed a new hydrogen isotope separation system, that combines water electrolysis and FCs [24]. Here, hydrogen and oxygen are produced by electrolysis and consumed by the FC. During hydrogen gas consumption in the FCs, power is generated and hydrogen isotopes are separated simultaneously. Previously we reported successful D separation using polymer electrolyte fuel cells (PEFCs) and alkaline exchange membrane FCs [25-27]. The mechanism of isotope separation is explained by the kinetic isotope effect (KIE). The separation reaction is discussed from the electrochemical elementary steps of oxidation and reduction reactions by a number of authors [28-30] and forms the basis for separation in both the electrolysis and fuel cell reactions.

However, although AFCs are potentially the lowest cost and most efficient fuel cell variant, the kinetic isotope effect in AFCs has not been investigated. In this paper, we employ Pt and Ru as the anode catalyst, respectively, and successfully separate D from mixtures of H₂ and D₂ gas. Several electrochemical techniques are applied to aid understanding of the separation mechanism.

2. Experimental

2-1. Preparation of Electrodes

The AFC gas diffusion layer (GDL) were made from its constituent components in our laboratory. Carbon black (Vulcan XC 72 R, Cabot, USA), activated charcoal (Norit, Sigma-Aldrich, UK) and carbon nanotube powder (NANOCYL NC 7000, Nanocyl, Belgium) were mixed in isopropyl alcohol to form a slurry. A wetproofing binder was added in the form of PTFE solution (60 wt% in

H₂O, Sigma-Aldrich) to give a paste like consistency. The homogeneous paste was calendared through rolls to a thickness of approximately 1 mm, dried and then laminated at 2,500 kg for 30 seconds onto a nickel mesh (4x4cm² perforated area). This gave a GDL and current collector assembly. Catalyst inks were prepared using a binder and solvent system consisting of PTFE, Texanol and Tergitol TMN6 (Sigma-Aldrich) solutions. The carbon -supported catalyst (10% Ru/C or 10% Pt/C, Alfa Aesar, USA) was added to this system to produce the final catalyst layer ink. These inks were then deposited on the GDL / current collector assembly by a screen printing method. The finished electrodes were cured at 250 °C in an oven for 10 minutes.

2-2. Electrochemical Measurements

A proprietary AFC test station (TS -11, AFC Energy Co., UK) which managed electrolyte and gas flows as well as temperature, was used for the experimental cell tests. Anode catalyst layers consisted of Ru or Pt catalyst, whereas the cathode was Pt in all cases. For the electrolyte fresh 5 M KOH solution was used each time. In the experimental procedure, after N₂ gas was introduced at 100 ml/min for 10 minutes, H₂ or D₂ gas was flowed at 20.0 ml/min to the anode. Air was flowed at 40 ml/min to the cathode. The cell temperature was controlled at 323 K. The voltage-current response of the cells were investigated by sweeping the cell current. A variable resistor (PLZ 164 WA, Kikusui Electronics Corp., Japan) was used to keep the current sweep rate of 20 mA/sec. The measurement was stopped when the output voltage reached 0.4 V or the current reached 1.5 A. Electrochemical impedance spectroscopy was employed to further understand the different responses using a frequency response analyzer (Solartron Analytical). These measurements were performed from 10 kHz to 0.1 Hz when the fuel cell was operating at a constant current of 0.5 A.

2-3. Separation Factor Measurement

A schematic diagram of the separation measurement is shown in Fig. 1. The flow rates of H₂ gas (15 ml/min) and D₂ gas (0.15 ml/min) were adjusted by mass flow controllers. They were mixed

and introduced into the anode. Pure O₂ gas (30 ml/min) was flown into the cathode. The hydrogen gas passing through the anode side was continuously sampled into a quadrupole mass spectrometer (QMS, Qulee-HGM 202, Ulvac Corp., Japan). The flow rate to the QMS was controlled with a needle valve to ensure that the total pressure in the chamber remained constant. The ion currents of the three gas species—with masses $m = 2, 3,$ and 4 representing H₂, HD, and D₂, respectively—were monitored.

3. Results and Discussion

3-1 Electrochemical Measurement

Two different types of AFC were examined; one with a Ru anode / Pt cathode (AFC_{Ru}), the other with a Pt anode / Pt cathode (AFC_{Pt}). The AFC performance was investigated when pure H₂ (red symbol) or D₂ gas (blue symbol) was supplied (Fig. 2). The open circuit voltages of both AFCs show about 1.03 V. No difference between isotopes is experienced at open circuit as expected. When the cells are connected across a load, the voltage was drops significantly as current is drawn. The large initial drop is attributed to the activation overvoltage by the nonequilibrium state. The drop value is about 0.13 V for AFC_{Ru} and 0.12 V for AFC_{Pt}.

Beyond this initial activation loss the cell voltages decrease proportional to the output current. This is explained by a resistive overvoltage, η_{ohm} [31]. The value is given by,

$$\eta_{\text{ohm}} = iR_{\text{ohm}} \quad (1)$$

where i is the current and R_{ohm} is the ohmic resistance of AFC. The R_{ohm} of AFC_{Ru} is 0.25 Ω for H₂ and 0.28 Ω for D₂ in the current range of 0.1 ~ 0.9 A. The AFC_{Pt} is more active and shows 0.18 Ω for both gases. The cell voltage of AFC_{Ru} show a large drop at currents greater than 1.3 A for H₂ and 1.0 A for D₂, as the cells approach a transport limit for gas diffusion in the GDL. At this point the insufficient gas supply increases the concentration overvoltage. The different onset of the voltage drop

indicates the slower D₂ diffusion in GDL.

The anode and the cathode potentials are measured using a reference electrode (Fig. 3). In each cell both cathode potentials (filled symbol) show almost the same behavior so difference in cell behavior can be attributed to the anode. The potential drop is confirmed as soon as the current draw is started. This initial drop is due to the sluggish oxygen reduction (ORR) kinetics experienced in all low temperature fuel cells. Beyond this point the cathode potentials decrease linearly with increasing current drawn. The ohmic resistances are about 0.12 Ω. The anode (opened symbol) does not show the potential jump having much more facile kinetics and increases linearly with increasing current (0.0 A ≤ *i* ≤ 0.5 A). The slope value depends on the gas type. The ohmic resistance for H₂ (0.14 Ω) is smaller than that for D₂ (0.16 Ω). When the current is more than 1.0 A, the potential sharply increases. This effect occurs at a smaller current for D₂ compared to H₂. This result is in agreement with the voltage drop due to the gas diffusion limitation, as seen in Fig. 2.

Electrochemical impedance measurements of the AFC anodes were measured. The data were collected during the power generation at 0.5 A. Figure 4 shows Nyquist plots of AFC_{Pt} (open symbol) and AFC_{Ru} (filled symbol). The AFC_{Pt} for H₂ (red plot) and D₂ (blue plot) shows the small semi-circular shape. They show almost same value of impedance of the right edge of the semi-circle at low frequency, which is equivalent to the charge transfer resistance. The small circle of AFC_{Pt} demonstrates the high catalytic activity for HOR, while AFC_{Ru} has a larger semi-circle which also varies with the gas type. The charge transfer resistance of D₂ is about 1.5 time as large as that of H₂.

3-2 D Isotope Separation

The D separation from a mixed gas of H₂ and D₂ was investigated. The mixing ratio of H and D was 1.0 at% D. The unreacted gas from the anode was introduced into the QMS. The ion currents of mass components (*i*_{H2}; *m* = 2, *i*_{HD}; *m* = 3, *i*_{D2}; *m* = 4) were measured at open circuit, before they were monitored during the AFC operation at 0.5 A.

Figure 5 shows the time variation of the ion currents of AFC_{Ru}. The D₂ form is changed into HD by passing through the anode. This is attributed to the exchange reaction, $H_2 + D_2 \rightarrow 2HD$, occurring on the catalyst. We have also confirmed this exchange reaction on PEFC anodes with Pt catalyst [26, 27].

When the AFC_{Ru} is put under load at 30 min after starting the measurement (arrow point in Fig. 5), the ion current, i_{H_2} , decreases from 2.0×10^{-8} A to 1.7×10^{-8} A by 120 min, while i_{D_2} increased from 3.1×10^{-12} A to 4.5×10^{-12} A. The value of i_{HD} does not change before or after the load is applied. It is noted that the ion current corresponds to the partial pressure of each compositions. By considering the reduction of i_{H_2} , the HD partial pressure actually increases relative to the H₂ one. Thus, the D atomic ratio in the gas increases during the power generation.

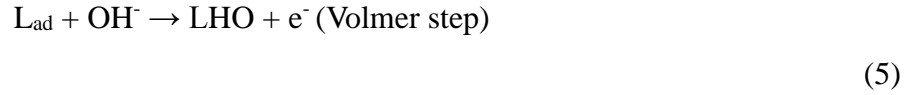
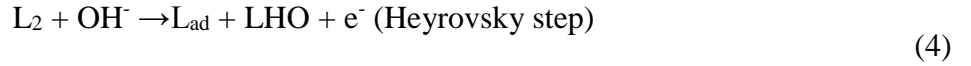
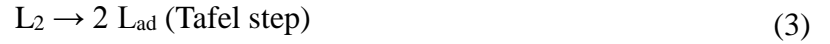
To evaluate the isotope separation, we calculate the separation factor, α , which compares the atomic ratios before/after the power generation phase. The value of α is defined by the following equation,

$$\alpha = ([H]/[D])_{\text{after}} / ([H]/[D])_{\text{before}} \quad (2)$$

where [H] and [D] represent atomic concentrations of H and D.

The α values of both AFCs are summarized in Table 1. The α of AFC_{Ru} is less than 1.0, meaning that H concentration in the anode exhaust gas is depleted, while D is enriched. However, the α of AFC_{Pt} is more than 1.0. In this case D is concentrated in the water produced by power generation. This is the opposite result compared to the Ru catalysts. For comparison, the α of PEFC using Pt catalyst is shown in Table 1 [26]. In PEFC with a Pt catalyst, the D isotope was also preferentially oxidized as experienced with the AFC_{Pt} results presented here.

The isotope separation was inversed between Ru and Pt [32]. The HOR consists of three elementary steps. When an alkali aqueous electrolyte is used, the steps are expressed by following;



Where L is symbol of H or D, and L_{ad} is a hydrogen atom adsorbed on the catalyst.

For Ru catalyst, the Tafel-Volmer combination is the main reaction path of hydrogen oxidation. The Volmer step with the charge transfer reaction is the rate determining [10, 33]. From the impedance results (Fig. 3), there is a significant difference in charge transfer resistance between H and D. Moreover, the desorption of hydrogen adatoms presumably contributes to the reaction rate of the Volmer step. The binding energy is -2.72 eV for H-Ru and -2.77 eV for D-Ru, respectively [34]. Since the desorption force of D-Ru is larger than that of H-Ru, D is not easily detached from the Ru catalyst surface. That is, the slow rate of D_{ad} detachment causes the less D_2 gas consumption, resulting in D enrichment in the gas exhausted from AFC_{Ru} . As another possibility, Ru adsorbs water molecules and hydronium ions more easily than Pt. If the adsorption tendency could be influenced by the mass number, the gas adsorption side at Eq. (3) would be blocked and the D_2 reaction rate might be reduced.

In the Pt catalyst case, Tafel-Volmer at low overpotential and Heyrovsky-Volmer at high overpotential occurs on the Pt catalyst [33]. Both Heyrovsky and Volmer steps, which accompany a charge transfer, hardly contribute to the isotope separation as illustrated by the Nyquist plots of H and D which are almost identical (Fig. 3). Therefore, the Tafel step may be important. The binding energy is -2.62 eV for H-Pt and -2.66 eV for D-Pt, respectively [34]. The reaction of D_2 with higher binding energy occurs preferentially at the Tafel step, where a gas molecule is dissociated and adsorbed on Pt atoms. Therefore, unlike the AFC_{Ru} results, more D_2 gas is consumed during AFC_{Pt} power generation.

4. Conclusions

This research demonstrates D separation using AFC_{Ru} and AFC_{Pt}. When the AFC_{Ru} is operated, the cell voltage when using D₂ as fuel is lower than that when using H₂. The impedance measurement indicates the larger charge transfer resistance for D compared to H, resulting in the slow oxidation reaction of D₂. The power performance of AFC_{Pt} is better than that of AFC_{Ru} and is not dependent on the gas species. The isotope separation was investigated when AFCs were operated at 0.5 A with using 1.0 at% D₂ mixture gas. The α value of AFC_{Ru} is 0.85 and D is enriched as product water, while α of AFC_{Pt} is 1.08. This inverse phenomenon, depending on the catalyst might be related to the differences in adsorption energy between the hydrogen atom and the catalyst surface for the two isotopes. The presented results demonstrate that the D concentration could be controlled by selecting proper catalysts. This will be meaningful knowledge for the isotope separation processes in the future.

Acknowledgments

The authors are grateful for financial support from the Ministry of Education, Culture, Sports, Science and Technology (Project No. 17H03528).

Figure Captions

Figure 1

Schematic illustration of isotope separation measurement using an alkaline fuel cell.

Figure 2

Current / cell voltage plots of alkaline fuel cell with Ru (●: AFC_{Ru}) and Pt (○: AFC_{Pt}) anode catalyst when supplying H₂ (red) and D₂ (blue) gas. (Temperature, 323 K; Cathode catalyst, Pt).

Figure 3

Current / potential plots of cathode (■) and anode (□) at AFC_{Ru} when supplying H₂ (red) and D₂ (blue) gas. (Temperature, 323 K; Cathode catalyst, Pt).

Figure 4

Complex plane plots for AFC_{Ru} (●) and AFC_{Pt} (○) when supplying H₂ (red) and D₂ (blue) gas. (Temperature, 323 K; Cathode catalyst, Pt).

Figure 5

Transient behavior of ionization currents of mass components (i_{H_2} ; red, i_{HD} ; blue, i_{D_2} ; green) during AFC_{Ru} operation at 0.5 A with 1.0 at% D₂ mixture gas.

Table 1 Separation factor, α , of AFC_{Ru}, AFC_{Pt} and PEMFC.

References

1. G. F. Mclean, T. Niet, S. Prince-Richard, N. Djilali, An assessment of alkaline fuel cell technology, *Int. J. Hydrog. Energy* 2002;27:507-526.
2. K. Kordesch, V. Hacker, J. Gsellmann, M. Cifrain, G. Faleschini, P. Enzinger, R. Fankhauser, M. Ortner, M. Muhr, R. R. Aronson, *J. Power Sources* 2000;86:162.
3. Z. F. Pan, R. Chen, L. An, Y. S. Li, *J. Power Sources*, **365** (2017) 430.
4. A. Verma, S. Basu, *J. Power Sources*, **168** (2007) 200.
5. E. Gülzow, M. Schulze U. Gerke, *J. Power Sources*, **156** (2006) 1.
6. J. Durst, A. Siebel, C. Simon, F. Hasché, J. Herranz, H. A. Gasteiger, *Energy Environ. Sci.*, **7** (2014) 2255.
7. W. Sheng, H. A. Gasteiger, Y. Shao-Horn, *J. Electrochem. Soc.*, **157** (2010) 1529.
8. K. J. P. Schouten, M. J. T. C. Van Der Niet, M. T. M. Koper, *Phys. Chem. Chem. Phys.*, **12** (2010) 15217.
9. X. P. Qin, L. L. Zhang, G. L. Xu, S. Q. Zhu, Q. Wang, M. Gu, X. Y. Zhang, C. J. Sun, P. B. Balbuena, K. Amine, M. H. Shao, *ACS Catal.*, **9** (2019) 9614.
10. J. K. Li, S. Ghoshal, M.K. Bates, T. E. Miller, V. Davies, E. Stavitski, K. Attenkofer, S. Mukerjee, Z. F. Ma, Q. Y. Jia, *Angew. Chemie - Int. Ed.*, **56** (2017) 15594.
11. R. Tanii, R. Ogawa, H. Matsushima, M. Ueda, *Int. J. Hydrog. Energy*, **44** (2019) 1851.
12. A. Pozio, S. Tosti, *Int. J. Hydrog. Energy*, **44** (2019) 7544.
13. S. Yanase, T. Oi, *J. Nucl. Sci. Technol.*, **50** (2013) 808.
14. D. Bessarabov, H. Wang, H. Li, N. Zhao ed., *PEM Electrolysis for Hydrogen Production*, CRC Press (2016) 361.
15. E. W. Washburn, H. C. Urey, *Proc. Natl. Acad. Sci. United States Am.*, **18** (1932) 496.
16. B. Topley, H. Eyring, *J. Chem. Phys.*, **2** (1934) 217.
17. R. Bhattacharyya, K. Bhanja, S. Mohan, *Int. J. Hydrog. Energy*, **41** (2016) 5003.
18. S. Fukada, *J. Nucl. Sci. Technol.*, **41** (2004) 619.
19. T. Sugiyama, Y. Asakura, T. Uda, Y. Abe, T. Shiozaki, Y. Enokida, I. Yamamoto, *J. Nucl. Sci. Technol.*, **41** (2004) 696.
20. K. Harada, R. Tanii, H. Matsushima, M. Ueda, K. Sato, T. Haneda, *Int. J. Hydrog. Energy*, **45** (2020) 31389.
21. D. Greenway, E. B. Fox, A. A. Ekechukwu, *Int. J. Hydrog. Energy*, **34** (2009) 6603.
22. D. L. Stojić, T. D. Grozdić, M. P. Marčeta Kaninski, A. D. Maksić, N. D. Simić, *Int. J. Hydrog. Energy*, **31** (2006) 841
23. F. Huang, C. Meng, *Int. J. Hydrog. Energy*, **35** (2010) 6108.
24. H. Matsushima, T. Nohira, T. Kitabata, Y. Ito, *Energy*, **30** (2005) 2413.
25. R. Ogawa, R. Tanii, R. Dawson, H. Matsushima, M. Ueda, *Energy*, **149** (2018) 98.
26. S. Shibuya, H. Matsushima, M. Ueda, *J. Electrochem. Soc.*, **163** (2016) F704.

27. R. Ogawa, H. Matsushima, M. Ueda, *Electrochem. Commun.*, **70** (2016) 5.
28. T. Y. George, T. Asset, A. Avid, P. Atanassov, I. V. Zenyuk, *ChemPhysChem.*, **21** (2020) 469.
29. D. Malko, A. Kucernak, *Electrochem. Commun.*, **83** (2017) 67.
30. M. Beltowska-Brzezinska, T. Luczak, J. Stelmach, R. Holze, *J. Power Sources*, **251** (2014) 30.
31. W. Phompan, N. Hansupalak, *J. Power Sources*, 196 (2011) 147.
32. E. C. M. Tse, T. T. H. Hoang, J. A. Varnell, A. A. Gewirth, *ACS Catal.*, **6** (2016) 5706.
33. K. Elbert, J. Hu, Z. Ma, Y. Zhang, G. Y. Chen, W. An, P. Liu, H. S. Isaacs, R. R. Adzic, J. X. Wang, *ACS Catal.*, **5** (2015) 6764.
34. Y. Bai, B. W. J. Chen, G. Peng, M. Mavrikakis, *Catal. Sci. Technol.*, **8** (2018) 3321.

Effect of Alkaline Fuel Cell Catalyst on Deuterium Isotope Separation

Risako Tani^{1z}, Ryota Ogawa¹, Hisayoshi Matsushima^{1*}, Mikito Ueda¹ and Richard Dawson²

¹Faculty of Engineering, Hokkaido University,

Kita 13 Nishi 8, Sapporo, Hokkaido 060-8628, Japan.

**Corresponding Author: matsushima@eng.hokudai.ac.jp*

Tel. & Fax +81-11-7066352

²Faculty of Engineering, Lancaster University,

Gillow Avenue, Lancaster LA1 4YW, UK.

^zNew Address; Toyota Motor Corporation,

Toyota-cho, Toyota, Aichi 471-8571, Japan.

Abstract

Fuel cells (FC) have been developed for automobiles and stationary power units. In addition to a power generator function, we propose a new application of hydrogen isotope separation. In this paper, deuterium (D) separation is investigated by two types of AFCs with platinum (Pt) or ruthenium (Ru) anode catalysts. The characteristics of the AFCs are evaluated by pure protium (H) or deuterium gas separately. In the case of Pt catalyst, the cell current/voltage curves show similar results for both gases. But a remarkable decrease in the voltage value is observed probably due to the mass transportation (diffusion) limitation at Ru catalyst. The limitation effect was larger for D₂ than H₂ gas. The AC impedance measurements supports that the slow reaction rate of D₂ gas on Ru catalyst. The separation experiments are verified with hydrogen gas mixed with 1 at% D. The D is diluted in the unreacted gas

discharged from AFC with Pt catalyst, but it is concentrated with Ru one. The inverse response may be attributed to the elementary process of the hydrogen oxidation reaction and the difference in the adsorption energy of gas and water molecules on the catalyst surface.

Keywords: Deuterium; Separation factor; Ruthenium; Fuel Cell; Hydrogen isotopes

1. Introduction

Hydrogen as an energy vector is very important for addressing world energy and environmental issues. Green hydrogen, in which carbon dioxide is not involved, is produced by water electrolysis and can then be utilized by FCs, thus providing a route to clean energy storage. Hence, when the primary electrical generation is via renewables such as wind, the system can be considered 'green'. The hydrogen energy society will be established in the automobile industry as one of the first main commercial applications.

There are several types of FCs which are usually classified by their electrolyte type. Alkaline fuel cells (AFCs) were the first variant to be developed for commercial usage and were employed in space applications due to their high reliability [1, 2]. These alkaline fuel cells used a liquid electrolyte but more recently, FCs using anion exchange membranes have been developed [3]. Alkaline fuel cells have an advantage of less cathode overpotential than other FCs allowing cells to be run at higher efficiencies. This also has significant impacts on cost, because AFCs can use non-precious catalysts or low precious metal loadings and inexpensive KOH as an electrolyte [4, 5]. However, the slow kinetic of hydrogen oxidation reaction (HOR) is still a problem [6-8]. It is reported that Pt-Ru alloy catalysts improve HOR and overtake the performance of Pt [9, 10]. Therefore, it is worthwhile investing Ru catalyst for HOR particularly as it is one of the least expensive platinum group metals.

Fuel cells have been much researched and developed as power devices, while the hydrogen isotopes separation as a new application has been explored although to a much lesser extent [11-14]. There exist three hydrogen isotopes: protium (H), deuterium (D) and tritium (T). D is used as a neutron moderator in heavy water reactors. The D-T reaction is involved in energy production in fusion reactors, which are expected to represent the next generation of nuclear energy. Therefore, large amounts of these isotopes are required for the energy industry. However, the separation and purification are difficult because of the similarity in physical and chemical properties. Research on hydrogen isotope

separation began in the 1930s [15, 16]. Many researchers have studied a variety of the separation methods, including water distillation [17, 18], chemical exchange [19], water electrolysis [20-22], and the combined electrolysis catalytic exchange (CECE) [23]. Electrolysis is the most efficient way, but it still has the disadvantage of high electricity consumption.

To overcome this drawback, the authors previously proposed a new hydrogen isotope separation system, that combines water electrolysis and FCs [24]. Here, hydrogen and oxygen are produced by electrolysis and consumed by the FC. During hydrogen gas consumption in the FCs, power is generated and hydrogen isotopes are separated simultaneously. Previously we reported successful D separation using polymer electrolyte fuel cells (PEFCs) and alkaline exchange membrane FCs [25-27]. The mechanism of isotope separation is explained by the kinetic isotope effect (KIE). The separation reaction is discussed from the electrochemical elementary steps of oxidation and reduction reactions by a number of authors [28-30] and forms the basis for separation in both the electrolysis and fuel cell reactions.

However, although AFCs are potentially the lowest cost and most efficient fuel cell variant, the isotope effect in AFCs has not been investigated. In this paper, we employ Pt and Ru as the anode catalyst, respectively, and successfully separate D from mixtures of H₂ and D₂ gas. Several electrochemical techniques are applied to aid understanding of the separation mechanism.

2. Experimental

2-1. Preparation of Electrodes

The AFC gas diffusion layer (GDL) were made from its constituent components in our laboratory. Carbon black (Vulcan XC 72 R, Cabot, USA), activated charcoal (Norit, Sigma-Aldrich, UK) and carbon nanotube powder (NANOCYL NC 7000, Nanocyl, Belgium) were mixed in isopropyl alcohol to form a slurry. A wetproofing binder was added in the form of PTFE solution (60 wt% in

H₂O, Sigma-Aldrich) to give a paste like consistency. The homogeneous paste was calendared through rolls to a thickness of approximately 1 mm, dried and then laminated at 2,500 kg for 30 seconds onto a nickel mesh (4x4cm² perforated area). This gave a GDL and current collector assembly. Catalyst inks were prepared using a binder and solvent system consisting of PTFE, Texanol and Tergitol TMN6 (Sigma-Aldrich) solutions. The carbon -supported catalyst (10% Ru/C or 10% Pt/C, Alfa Aesar, USA) was added to this system to produce the final catalyst layer ink. These inks were then deposited on the GDL / current collector assembly by a screen printing method. The finished electrodes were cured at 250 °C in an oven for 10 minutes.

2-2. Electrochemical Measurements

A proprietary AFC test station (TS -11, AFC Energy Co., UK) which managed electrolyte and gas flows as well as temperature, was used for the experimental cell tests. Anode catalyst layers consisted of Ru or Pt catalyst, whereas the cathode was Pt in all cases. For the electrolyte fresh 5 M KOH solution was used each time. In the experimental procedure, after N₂ gas was introduced at 100 ml/min for 10 minutes, H₂ or D₂ gas was flowed at 20.0 ml/min to the anode. Air was flowed at 40 ml/min to the cathode. The cell temperature was controlled at 323 K. The voltage-current response of the cells were investigated by sweeping the cell current. A variable resistor (PLZ 164 WA, Kikusui Electronics Corp., Japan) was used to keep the current sweep rate of 20 mA/sec. The measurement was stopped when the output voltage reached 0.4 V or the current reached 1.5 A. Electrochemical impedance spectroscopy was employed to further understand the different responses using a frequency response analyzer (Solartron Analytical). These measurements were performed from 10 kHz to 0.1 Hz when the fuel cell was operating at a constant current of 0.5 A.

2-3. Separation Factor Measurement

A schematic diagram of the separation measurement is shown in Fig. 1. The flow rates of H₂ gas (15 ml/min) and D₂ gas (0.15 ml/min) were adjusted by mass flow controllers. They were mixed

and introduced into the anode. Pure O₂ gas (30 ml/min) was flown into the cathode. The hydrogen gas passing through the anode side was continuously sampled into a quadrupole mass spectrometer (QMS, Qulee-HGM 202, Ulvac Corp., Japan). The flow rate to the QMS was controlled with a needle valve to ensure that the total pressure in the chamber remained constant. The ion currents of the three gas species—with masses $m = 2, 3,$ and 4 representing H₂, HD, and D₂, respectively—were monitored.

3. Results and Discussion

3-1 Electrochemical Measurement

Two different types of AFC were examined; one with a Ru anode / Pt cathode (AFC_{Ru}), the other with a Pt anode / Pt cathode (AFC_{Pt}). The AFC performance was investigated when pure H₂ (red symbol) or D₂ gas (blue symbol) was supplied (Fig. 2). The open circuit voltages of both AFCs show about 1.03 V. No difference between isotopes is experienced at open circuit as expected. When the cells are connected across a load, the voltage was drops significantly as current is drawn. The large initial drop is attributed to the activation overvoltage by the nonequilibrium state. The drop value is about 0.13 V for AFC_{Ru} and 0.12 V for AFC_{Pt}.

Beyond this initial activation loss the cell voltages decrease proportional to the output current. This is explained by a resistive overvoltage, η_{ohm} [31]. The value is given by,

$$\eta_{\text{ohm}} = iR_{\text{ohm}} \quad (1)$$

where i is the current and R_{ohm} is the ohmic resistance of AFC. The R_{ohm} of AFC_{Ru} is 0.25 Ω for H₂ and 0.28 Ω for D₂ in the current range of 0.1 ~ 0.9 A. The AFC_{Pt} is more active and shows 0.18 Ω for both gases. The cell voltage of AFC_{Ru} show a large drop at currents greater than 1.3 A for H₂ and 1.0 A for D₂, as the cells approach a transport limit for gas diffusion in the GDL. At this point the insufficient gas supply increases the concentration overvoltage. The different onset of the voltage drop

indicates the slower D₂ diffusion in GDL.

The anode and the cathode potentials are measured using a reference electrode (Fig. 3). In each cell both cathode potentials (filled symbol) show almost the same behavior so difference in cell behavior can be attributed to the anode. The potential drop is confirmed as soon as the current draw is started. This initial drop is due to the sluggish oxygen reduction (ORR) kinetics experienced in all low temperature fuel cells. Beyond this point the cathode potentials decrease linearly with increasing current drawn. The ohmic resistances are about 0.12 Ω. The anode (opened symbol) does not show the potential jump having much more facile kinetics and increases linearly with increasing current (0.0 A ≤ *i* ≤ 0.5 A). The slope value depends on the gas type. The ohmic resistance for H₂ (0.14 Ω) is smaller than that for D₂ (0.16 Ω). When the current is more than 1.0 A, the potential sharply increases. This effect occurs at a smaller current for D₂ compared to H₂. This result is in agreement with the voltage drop due to the gas diffusion limitation, as seen in Fig. 2.

Electrochemical impedance measurements of the AFC anodes were measured. The data were collected during the power generation at 0.5 A. Figure 4 shows Nyquist plots of AFC_{Pt} (open symbol) and AFC_{Ru} (filled symbol). The AFC_{Pt} for H₂ (red plot) and D₂ (blue plot) shows the small semi-circular shape. They show almost same value of impedance of the right edge of the semi-circle at low frequency, which is equivalent to the charge transfer resistance. The small circle of AFC_{Pt} demonstrates the high catalytic activity for HOR, while AFC_{Ru} has a larger semi-circle which also varies with the gas type. The charge transfer resistance of D₂ is about 1.5 time as large as that of H₂.

3-2 D Isotope Separation

The D separation from a mixed gas of H₂ and D₂ was investigated. The mixing ratio of H and D was 1.0 at% D. The unreacted gas from the anode was introduced into the QMS. The ion currents of mass components (*i*_{H2}; *m* = 2, *i*_{HD}; *m* = 3, *i*_{D2}; *m* = 4) were measured at open circuit, before they were monitored during the AFC operation at 0.5 A.

Figure 5 shows the time variation of the ion currents of AFC_{Ru}. The D₂ form is changed into HD by passing through the anode. This is attributed to the exchange reaction, $H_2 + D_2 \rightarrow 2HD$, occurring on the catalyst. We have also confirmed this exchange reaction on PEFC anodes with Pt catalyst [26, 27].

When the AFC_{Ru} is put under load at 30 min after starting the measurement (arrow point in Fig. 5), the ion current, i_{H_2} , decreases from 2.0×10^{-8} A to 1.7×10^{-8} A by 120 min, while i_{D_2} increased from 3.1×10^{-12} A to 4.5×10^{-12} A. The value of i_{HD} does not change before or after the load is applied. It is noted that the ion current corresponds to the partial pressure of each compositions. By considering the reduction of i_{H_2} , the HD partial pressure actually increases relative to the H₂ one. Thus, the D atomic ratio in the gas increases during the power generation.

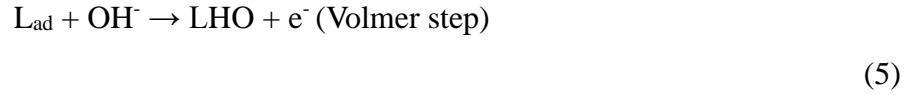
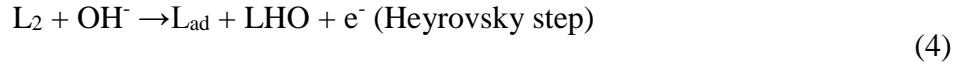
To evaluate the isotope separation, we calculate the separation factor, α , which compares the atomic ratios before/after the power generation phase. The value of α is defined by the following equation,

$$\alpha = ([H]/[D])_{\text{after}}/([H]/[D])_{\text{before}} \quad (2)$$

where [H] and [D] represent atomic concentrations of H and D.

The α values of both AFCs are summarized in Table 1. The α of AFC_{Ru} is less than 1.0, meaning that H concentration in the anode exhaust gas is depleted, while D is enriched. However, the α of AFC_{Pt} is more than 1.0. In this case D is concentrated in the water produced by power generation. This is the opposite result compared to the Ru catalysts. For comparison, the α of PEFC using Pt catalyst is shown in Table 1 [26]. In PEFC with a Pt catalyst, the D isotope was also preferentially oxidized as experienced with the AFC_{Pt} results presented here.

The isotope separation was inversed between Ru and Pt [32]. The HOR consists of three elementary steps. When an alkali aqueous electrolyte is used, the steps are expressed by following;



Where L is symbol of H or D, and L_{ad} is a hydrogen atom adsorbed on the catalyst.

For Ru catalyst, the Tafel-Volmer combination is the main reaction path of hydrogen oxidation. The Volmer step with the charge transfer reaction is the rate determining [10, 33]. From the impedance results (Fig. 3), there is a significant difference in charge transfer resistance between H and D. Moreover, the desorption of hydrogen adatoms presumably contributes to the reaction rate of the Volmer step. The binding energy is -2.72 eV for H-Ru and -2.77 eV for D-Ru, respectively [34]. Since the desorption force of D-Ru is larger than that of H-Ru, D is not easily detached from the Ru catalyst surface. That is, the slow rate of D_{ad} detachment causes the less D_2 gas consumption, resulting in D enrichment in the gas exhausted from AFC_{Ru}. As another possibility, Ru adsorbs water molecules and hydronium ions more easily than Pt. If the adsorption tendency could be influenced by the mass number, the gas adsorption side at Eq. (3) would be blocked and the D_2 reaction rate might be reduced.

In the Pt catalyst case, Tafel-Volmer at low overpotential and Heyrovsky-Volmer at high overpotential occurs on the Pt catalyst [33]. Both Heyrovsky and Volmer steps, which accompany a charge transfer, hardly contribute to the isotope separation as illustrated by the Nyquist plots of H and D which are almost identical (Fig. 3). Therefore, the Tafel step may be important. The binding energy is -2.62 eV for H-Pt and -2.66 eV for D-Pt, respectively [34]. The reaction of D_2 with higher binding energy occurs preferentially at the Tafel step, where a gas molecule is dissociated and adsorbed on Pt atoms. Therefore, unlike the AFC_{Ru} results, more D_2 gas is consumed during AFC_{Pt} power generation.

4. Conclusions

This research demonstrates D separation using AFC_{Ru} and AFC_{Pt}. When the AFC_{Ru} is operated, the cell voltage when using D₂ as fuel is lower than that when using H₂. The impedance measurement indicates the larger charge transfer resistance for D compared to H, resulting in the slow oxidation reaction of D₂. The power performance of AFC_{Pt} is better than that of AFC_{Ru} and is not dependent on the gas species. The isotope separation was investigated when AFCs were operated at 0.5 A with using 1.0 at% D₂ mixture gas. The α value of AFC_{Ru} is 0.85 and D is enriched as product water, while α of AFC_{Pt} is 1.08. This inverse phenomenon, depending on the catalyst might be related to the differences in adsorption energy between the hydrogen atom and the catalyst surface for the two isotopes. The presented results demonstrate that the D concentration could be controlled by selecting proper catalysts. This will be meaningful knowledge for the isotope separation processes in the field of fusion reactor and material development [35-37].

Acknowledgments

The authors are grateful for financial support from the Ministry of Education, Culture, Sports, Science and Technology (Project No. 17H03528).

Figure Captions

Figure 1

Schematic illustration of isotope separation measurement using an alkaline fuel cell.

Figure 2

Current / cell voltage plots of alkaline fuel cell with Ru (●: AFC_{Ru}) and Pt (○: AFC_{Pt}) anode catalyst when supplying H₂ (red) and D₂ (blue) gas. (Temperature, 323 K; Cathode catalyst, Pt).

Figure 3

Current / potential plots of cathode (■) and anode (□) at AFC_{Ru} when supplying H₂ (red) and D₂ (blue) gas. (Temperature, 323 K; Cathode catalyst, Pt).

Figure 4

Complex plane plots for AFC_{Ru} (●) and AFC_{Pt} (○) when supplying H₂ (red) and D₂ (blue) gas. (Temperature, 323 K; Cathode catalyst, Pt).

Figure 5

Transient behavior of ionization currents of mass components (i_{H_2} ; red, i_{HD} ; blue, i_{D_2} ; green) during AFC_{Ru} operation at 0.5 A with 1.0 at% D₂ mixture gas.

Table 1 Separation factor, α , of AFC_{Ru}, AFC_{Pt} and PEMFC.

References

1. G. F. Mclean, T. Niet, S. Prince-Richard, N. Djilali, An assessment of alkaline fuel cell technology, *Int. J. Hydrog. Energy* 2002;27:507-526.
2. K. Kordesch, V. Hacker, J. Gsellmann, M. Cifrain, G. Faleschini, P. Enzinger, R. Fankhauser, M. Ortner, M. Muhr, R. R. Aronson, Alkaline fuel cells applications, *J. Power Sources* 2000;86:162-165.
3. Z. F. Pan, R. Chen, L. An, Y. S. Li, Alkaline anion exchange membrane fuel cells for cogeneration of electricity and valuable chemicals, *J. Power Sources* 2017;365:430-445.
4. A. Verma, S. Basu, Experimental evaluation and mathematical modeling of a direct alkaline fuel cell, *J. Power Sources* 2007;168:200-210.
5. E. Gülzow, M. Schulze U. Gerke, Bipolar concept for alkaline fuel cells, *J. Power Sources* 2006;156:1-7.
6. J. Durst, A. Siebel, C. Simon, F. Hasché, J. Herranz, H. A. Gasteiger, New insights into the electrochemical hydrogen oxidation and evolution reaction mechanism, *Energy Environ. Sci.* 2014;7:2255-2260.
7. W. Sheng, H. A. Gasteiger, Y. Shao-Horn, Hydrogen Oxidation and Evolution Reaction Kinetics on Platinum: Acid vs Alkaline Electrolytes, *J. Electrochem. Soc.* 2010;157:B1529-B1536.
8. K. J. P. Schouten, M. J. T. C. Van Der Niet, M. T. M. Koper, Impedance spectroscopy of H and OH adsorption on stepped single-crystal platinum electrodes in alkaline and acidic media, *Phys. Chem. Chem. Phys.* 2010;12:15217-15224.
9. X. P. Qin, L. L. Zhang, G. L. Xu, S. Q. Zhu, Q. Wang, M. Gu, X. Y. Zhang, C. J. Sun, P. B. Balbuena, K. Amine, M. H. Shao, The Role of Ru in Improving the Activity of Pd toward Hydrogen Evolution and Oxidation Reactions in Alkaline Solutions, *ACS Catal.* 2019;9:9614-9621.
10. J. K. Li, S. Ghoshal, M.K. Bates, T. E. Miller, V. Davies, E. Stavitski, K. Attenkofer, S. Mukerjee, Z. F. Ma, Q. Y. Jia, Experimental Proof of the Bifunctional Mechanism for the Hydrogen Oxidation in Alkaline Media, *Angew. Chemie - Int. Ed.* 2017;56:15594-15598.
11. R. Tanii, R. Ogawa, H. Matsushima, M. Ueda, Measurement of deuterium isotope separation by polymer electrolyte fuel cell stack, *Int. J. Hydrog. Energy* 2019;44:1851-1856.
12. A. Pozio, S. Tosti, Isotope effects H/D in a PEFC with Pt-Ru/anode at low and high current density, *Int. J. Hydrog. Energy* 2019;44:7544-7554.
13. S. Yanase, T. Oi, Observation of H/D isotope effects on polymer electrolyte membrane fuel cell operations, *J. Nucl. Sci. Technol.* 2013;50:808-812.
14. D. Bessarabov, H. Wang, H. Li, N. Zhao ed., *PEM Electrolysis for Hydrogen Production*, CRC Press 2016:361.
15. E. W. Washburn, H. C. Urey, Concentration of the H-2 isotope of hydrogen by the fractional

- electrolysis of water *Proc. Natl. Acad. Sci. United States Am.* 1932;18:496-498.
16. B. Topley, H. Eyring, The Separation of the Hydrogen Isotopes by Electrolysis, *J. Chem. Phys.* 1934;2:217-230.
 17. R. Bhattacharyya, K. Bhanja, S. Mohan, Simulation studies of the characteristics of a cryogenic distillation column for hydrogen isotope separation, *Int. J. Hydrog. Energy* 2016;41:5003-5018.
 18. S. Fukada, Tritium Isotope Separation by Water Distillation Column Packed with Silica-gel Beads, *J. Nucl. Sci. Technol.* 2004;41:619-623.
 19. T. Sugiyama, Y. Asakura, T. Uda, Y. Abe, T. Shiozaki, Y. Enokida, I. Yamamoto, Preliminary Experiments on Hydrogen Isotope Separation by Water-Hydrogen Chemical Exchange under Reduced Pressure, *J. Nucl. Sci. Technol.* 2004;41:696-701.
 20. K. Harada, R. Tanii, H. Matsushima, M. Ueda, K. Sato, T. Haneda, Effects of water transport on deuterium isotope separation during polymer electrolyte membrane water electrolysis, *Int. J. Hydrog. Energy* 2020;45:31389-31395.
 21. D. Greenway, E. B. Fox, A. A. Ekechukwu, Proton exchange membrane (PEM) electrolyzer operation under anode liquid and cathode vapor feed configurations, *Int. J. Hydrog. Energy* 2009;34:6603-6608.
 22. D. L. Stojić, T. D. Grozdić, M. P. Marčeta Kaninski, A. D. Maksić, N. D. Simić, Intermetallics as advanced cathode materials in hydrogen production via electrolysis, *Int. J. Hydrog. Energy* 2006;31:841-846.
 23. F. Huang, C. Meng, Hydrophobic platinum–polytetrafluoroethylene catalyst for hydrogen isotope separation, *Int. J. Hydrog. Energy* 2010;35:6108-6112.
 24. H. Matsushima, T. Nohira, T. Kitabata, Y. Ito, A novel deuterium separation system by the combination of water electrolysis and fuel cell, *Energy* 2005;30:2413-2423.
 25. R. Ogawa, R. Tanii, R. Dawson, H. Matsushima, M. Ueda, Deuterium isotope separation by combined electrolysis fuel cell, *Energy* 2018;149:98-104.
 26. S. Shibuya, H. Matsushima, M. Ueda, Study of Deuterium Isotope Separation by PEFC, *J. Electrochem. Soc.* 2016;163:F704-F707.
 27. R. Ogawa, H. Matsushima, M. Ueda, Hydrogen isotope separation with an alkaline membrane fuel cell, *Electrochem. Commun.* 2016;70:5-7.
 28. T. Y. George, T. Asset, A. Avid, P. Atanassov, I. V. Zenyuk, Kinetic Isotope Effect as a Tool To Investigate the Oxygen Reduction Reaction on Pt-based Electrocatalysts - Part I: High-loading Pt/C and Pt Extended Surface, *ChemPhysChem.* 2020;21:469-475.
 29. D. Malko, A. Kucernak, Kinetic isotope effect in the oxygen reduction reaction (ORR) over Fe-N/C catalysts under acidic and alkaline conditions, *Electrochem. Commun.* 2017;83:67-71.
 30. M. Beltowska-Brzezinska, T. Luczak, J. Stelmach, R. Holze, The electrooxidation mechanism

- of formic acid on platinum and on lead ad-atoms modified platinum studied with the kinetic isotope effect, *J. Power Sources* 2014;251:30-37.
31. W. Phompan, N. Hansupalak, Improvement of proton-exchange membrane fuel cell performance using platinum-loaded carbon black entrapped in crosslinked chitosan, *J. Power Sources* 2011;196:147-152.
 32. E. C. M. Tse, T. T. H. Hoang, J. A. Varnell, A. A. Gewirth, Observation of an Inverse Kinetic Isotope Effect in Oxygen Evolution Electrochemistry, *ACS Catal.* 2016;6:5706-5714.
 33. K. Elbert, J. Hu, Z. Ma, Y. Zhang, G. Y. Chen, W. An, P. Liu, H. S. Isaacs, R. R. Adzic, J. X. Wang, Elucidating Hydrogen Oxidation/Evolution Kinetics in Base and Acid by Enhanced Activities at the Optimized Pt Shell Thickness on the Ru Core, *ACS Catal* 2015;5:6764-6772.
 34. Y. Bai, B. W. J. Chen, G. Peng, M. Mavrikakis, Density functional theory study of thermodynamic and kinetic isotope effects of H-2/D-2 dissociative adsorption on transition metals, *Catal. Sci. Technol.* 2018;8:3321-3335.
 35. M. Y. Yang, J. B. Zhou, L. P. Gao, The purification of hydrogen isotopes expelled from nuclear fusion reactors by a combined process, *Int. J. Hydrog. Energy* 2020;45:13596-13600.
 36. W. J. Byeon, S. K. Lee, S. J. Noh, Transport of hydrogen and deuterium in 316LN stainless steel over a wide temperature range for nuclear hydrogen and nuclear fusion applications, *Int. J. Hydrog. Energy* 2020;45:8827-8832.
 37. M. Glugla, R. Lasser, L. Dorr, D. K. Murdoch, R. Haange, H. Yoshida, The inner deuterium/tritium fuel cycle of ITER, *Fusion Eng. Des.* 2003;69:39-43.

Effect of Alkaline Fuel Cell Catalyst on Deuterium Isotope Separation

Risako Tanii^{1z}, Ryota Ogawa¹, Hisayoshi Matsushima^{1*}, Mikito Ueda¹ and Richard Dawson²

¹Faculty of Engineering, Hokkaido University,

Kita 13 Nishi 8, Sapporo, Hokkaido 060-8628, Japan.

**Corresponding Author: matsushima@eng.hokudai.ac.jp*

Tel. & Fax +81-11-7066352

²Faculty of Engineering, Lancaster University,

Gillow Avenue, Lancaster LA1 4YW, UK.

^zNew Address; Toyota Motor Corporation,

Toyota-cho, Toyota, Aichi 471-8571, Japan.

Abstract

Fuel cells (FC) have been developed for automobiles and stationary power units. In addition to a power generator function, we propose a new application of hydrogen isotope separation. In this paper, deuterium (D) separation is investigated by two types of AFCs with platinum (Pt) or ruthenium (Ru) anode catalysts. The characteristics of the AFCs are evaluated by pure protium (H) or deuterium gas separately. In the case of Pt catalyst, the cell current/voltage curves show similar results for both gases. But a remarkable decrease in the voltage value is observed probably due to the mass transportation (diffusion) limitation at Ru catalyst. The limitation effect was larger for D₂ than H₂ gas. The AC impedance measurements supports that the slow reaction rate of D₂ gas on Ru catalyst. The separation experiments are verified with hydrogen gas mixed with 1 at% D. The D is diluted in the unreacted gas

discharged from AFC with Pt catalyst, but it is concentrated with Ru one. The inverse response may be attributed to the elementary process of the hydrogen oxidation reaction and the difference in the adsorption energy of gas and water molecules on the catalyst surface.

Keywords: Deuterium; Separation factor; Ruthenium; Fuel Cell; Hydrogen isotopes

1. Introduction

Hydrogen as an energy vector is very important for addressing world energy and environmental issues. Green hydrogen, in which carbon dioxide is not involved, is produced by water electrolysis and can then be utilized by FCs, thus providing a route to clean energy storage. Hence, when the primary electrical generation is via renewables such as wind, the system can be considered 'green'. The hydrogen energy society will be established in the automobile industry as one of the first main commercial applications.

There are several types of FCs which are usually classified by their electrolyte type. Alkaline fuel cells (AFCs) were the first variant to be developed for commercial usage and were employed in space applications due to their high reliability [1, 2]. These alkaline fuel cells used a liquid electrolyte but more recently, FCs using anion exchange membranes have been developed [3]. Alkaline fuel cells have an advantage of less cathode overpotential than other FCs allowing cells to be run at higher efficiencies. This also has significant impacts on cost, because AFCs can use non-precious catalysts or low precious metal loadings and inexpensive KOH as an electrolyte [4, 5]. However, the slow kinetic of hydrogen oxidation reaction (HOR) is still a problem [6-8]. It is reported that Pt-Ru alloy catalysts improve HOR and overtake the performance of Pt [9, 10]. Therefore, it is worthwhile investing Ru catalyst for HOR particularly as it is one of the least expensive platinum group metals.

Fuel cells have been much researched and developed as power devices, while the hydrogen isotopes separation as a new application has been explored although to a much lesser extent [11-14]. There exist three hydrogen isotopes: protium (H), deuterium (D) and tritium (T). D is used as a neutron moderator in heavy water reactors. The D-T reaction is involved in energy production in fusion reactors, which are expected to represent the next generation of nuclear energy. Therefore, large amounts of these isotopes are required for the energy industry. However, the separation and purification are difficult because of the similarity in physical and chemical properties. Research on hydrogen isotope

separation began in the 1930s [15, 16]. Many researchers have studied a variety of the separation methods, including water distillation [17, 18], chemical exchange [19], water electrolysis [20-22], and the combined electrolysis catalytic exchange (CECE) [23]. Electrolysis is the most efficient way, but it still has the disadvantage of high electricity consumption.

To overcome this drawback, the authors previously proposed a new hydrogen isotope separation system, that combines water electrolysis and FCs [24]. Here, hydrogen and oxygen are produced by electrolysis and consumed by the FC. During hydrogen gas consumption in the FCs, power is generated and hydrogen isotopes are separated simultaneously. Previously we reported successful D separation using polymer electrolyte fuel cells (PEFCs) and alkaline exchange membrane FCs [25-27]. The mechanism of isotope separation is explained by the kinetic isotope effect (KIE). The separation reaction is discussed from the electrochemical elementary steps of oxidation and reduction reactions by a number of authors [28-30] and forms the basis for separation in both the electrolysis and fuel cell reactions.

However, although AFCs are potentially the lowest cost and most efficient fuel cell variant, the isotope effect in AFCs has not been investigated. In this paper, we employ Pt and Ru as the anode catalyst, respectively, and successfully separate D from mixtures of H₂ and D₂ gas. Several electrochemical techniques are applied to aid understanding of the separation mechanism.

2. Experimental

2-1. Preparation of Electrodes

The AFC gas diffusion layer (GDL) were made from its constituent components in our laboratory. Carbon black (Vulcan XC 72 R, Cabot, USA), activated charcoal (Norit, Sigma-Aldrich, UK) and carbon nanotube powder (NANOCYL NC 7000, Nanocyl, Belgium) were mixed in isopropyl alcohol to form a slurry. A wetproofing binder was added in the form of PTFE solution (60 wt% in

H₂O, Sigma-Aldrich) to give a paste like consistency. The homogeneous paste was calendared through rolls to a thickness of approximately 1 mm, dried and then laminated at 2,500 kg for 30 seconds onto a nickel mesh (4x4cm² perforated area). This gave a GDL and current collector assembly. Catalyst inks were prepared using a binder and solvent system consisting of PTFE, Texanol and Tergitol TMN6 (Sigma-Aldrich) solutions. The carbon -supported catalyst (10% Ru/C or 10% Pt/C, Alfa Aesar, USA) was added to this system to produce the final catalyst layer ink. These inks were then deposited on the GDL / current collector assembly by a screen printing method. The finished electrodes were cured at 250 °C in an oven for 10 minutes.

2-2. Electrochemical Measurements

A proprietary AFC test station (TS -11, AFC Energy Co., UK) which managed electrolyte and gas flows as well as temperature, was used for the experimental cell tests. Anode catalyst layers consisted of Ru or Pt catalyst, whereas the cathode was Pt in all cases. For the electrolyte fresh 5 M KOH solution was used each time. In the experimental procedure, after N₂ gas was introduced at 100 ml/min for 10 minutes, H₂ or D₂ gas was flowed at 20.0 ml/min to the anode. Air was flowed at 40 ml/min to the cathode. The cell temperature was controlled at 323 K. The voltage-current response of the cells were investigated by sweeping the cell current. A variable resistor (PLZ 164 WA, Kikusui Electronics Corp., Japan) was used to keep the current sweep rate of 20 mA/sec. The measurement was stopped when the output voltage reached 0.4 V or the current reached 1.5 A. Electrochemical impedance spectroscopy was employed to further understand the different responses using a frequency response analyzer (Solartron Analytical). These measurements were performed from 10 kHz to 0.1 Hz when the fuel cell was operating at a constant current of 0.5 A.

2-3. Separation Factor Measurement

A schematic diagram of the separation measurement is shown in Fig. 1. The flow rates of H₂ gas (15 ml/min) and D₂ gas (0.15 ml/min) were adjusted by mass flow controllers. They were mixed

and introduced into the anode. Pure O₂ gas (30 ml/min) was flown into the cathode. The hydrogen gas passing through the anode side was continuously sampled into a quadrupole mass spectrometer (QMS, Qulee-HGM 202, Ulvac Corp., Japan). The flow rate to the QMS was controlled with a needle valve to ensure that the total pressure in the chamber remained constant. The ion currents of the three gas species—with masses $m = 2, 3,$ and 4 representing H₂, HD, and D₂, respectively—were monitored.

3. Results and Discussion

3-1 Electrochemical Measurement

Two different types of AFC were examined; one with a Ru anode / Pt cathode (AFC_{Ru}), the other with a Pt anode / Pt cathode (AFC_{Pt}). The AFC performance was investigated when pure H₂ (red symbol) or D₂ gas (blue symbol) was supplied (Fig. 2). The open circuit voltages of both AFCs show about 1.03 V. No difference between isotopes is experienced at open circuit as expected. When the cells are connected across a load, the voltage was drops significantly as current is drawn. The large initial drop is attributed to the activation overvoltage by the nonequilibrium state. The drop value is about 0.13 V for AFC_{Ru} and 0.12 V for AFC_{Pt}.

Beyond this initial activation loss the cell voltages decrease proportional to the output current. This is explained by a resistive overvoltage, η_{ohm} [31]. The value is given by,

$$\eta_{\text{ohm}} = iR_{\text{ohm}} \quad (1)$$

where i is the current and R_{ohm} is the ohmic resistance of AFC. The R_{ohm} of AFC_{Ru} is 0.25 Ω for H₂ and 0.28 Ω for D₂ in the current range of 0.1 ~ 0.9 A. The AFC_{Pt} is more active and shows 0.18 Ω for both gases. The cell voltage of AFC_{Ru} show a large drop at currents greater than 1.3 A for H₂ and 1.0 A for D₂, as the cells approach a transport limit for gas diffusion in the GDL. At this point the insufficient gas supply increases the concentration overvoltage. The different onset of the voltage drop

indicates the slower D₂ diffusion in GDL.

The anode and the cathode potentials are measured using a reference electrode (Fig. 3). In each cell both cathode potentials (filled symbol) show almost the same behavior so difference in cell behavior can be attributed to the anode. The potential drop is confirmed as soon as the current draw is started. This initial drop is due to the sluggish oxygen reduction (ORR) kinetics experienced in all low temperature fuel cells. Beyond this point the cathode potentials decrease linearly with increasing current drawn. The ohmic resistances are about 0.12 Ω. The anode (opened symbol) does not show the potential jump having much more facile kinetics and increases linearly with increasing current (0.0 A ≤ *i* ≤ 0.5 A). The slope value depends on the gas type. The ohmic resistance for H₂ (0.14 Ω) is smaller than that for D₂ (0.16 Ω). When the current is more than 1.0 A, the potential sharply increases. This effect occurs at a smaller current for D₂ compared to H₂. This result is in agreement with the voltage drop due to the gas diffusion limitation, as seen in Fig. 2.

Electrochemical impedance measurements of the AFC anodes were measured. The data were collected during the power generation at 0.5 A. Figure 4 shows Nyquist plots of AFC_{Pt} (open symbol) and AFC_{Ru} (filled symbol). The AFC_{Pt} for H₂ (red plot) and D₂ (blue plot) shows the small semi-circular shape. They show almost same value of impedance of the right edge of the semi-circle at low frequency, which is equivalent to the charge transfer resistance. The small circle of AFC_{Pt} demonstrates the high catalytic activity for HOR, while AFC_{Ru} has a larger semi-circle which also varies with the gas type. The charge transfer resistance of D₂ is about 1.5 time as large as that of H₂.

3-2 D Isotope Separation

The D separation from a mixed gas of H₂ and D₂ was investigated. The mixing ratio of H and D was 1.0 at% D. The unreacted gas from the anode was introduced into the QMS. The ion currents of mass components (*i*_{H2}; *m* = 2, *i*_{HD}; *m* = 3, *i*_{D2}; *m* = 4) were measured at open circuit, before they were monitored during the AFC operation at 0.5 A.

Figure 5 shows the time variation of the ion currents of AFC_{Ru}. The D₂ form is changed into HD by passing through the anode. This is attributed to the exchange reaction, $H_2 + D_2 \rightarrow 2HD$, occurring on the catalyst. We have also confirmed this exchange reaction on PEFC anodes with Pt catalyst [26, 27].

When the AFC_{Ru} is put under load at 30 min after starting the measurement (arrow point in Fig. 5), the ion current, i_{H_2} , decreases from 2.0×10^{-8} A to 1.7×10^{-8} A by 120 min, while i_{D_2} increased from 3.1×10^{-12} A to 4.5×10^{-12} A. The value of i_{HD} does not change before or after the load is applied. It is noted that the ion current corresponds to the partial pressure of each compositions. By considering the reduction of i_{H_2} , the HD partial pressure actually increases relative to the H₂ one. Thus, the D atomic ratio in the gas increases during the power generation.

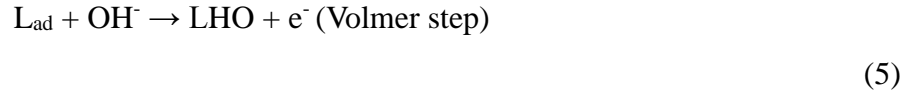
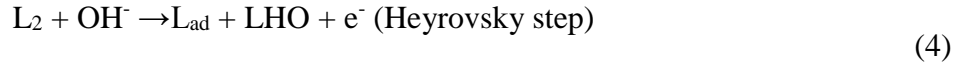
To evaluate the isotope separation, we calculate the separation factor, α , which compares the atomic ratios before/after the power generation phase. The value of α is defined by the following equation,

$$\alpha = ([H]/[D])_{\text{after}}/([H]/[D])_{\text{before}} \quad (2)$$

where [H] and [D] represent atomic concentrations of H and D.

The α values of both AFCs are summarized in Table 1. The α of AFC_{Ru} is less than 1.0, meaning that H concentration in the anode exhaust gas is depleted, while D is enriched. However, the α of AFC_{Pt} is more than 1.0. In this case D is concentrated in the water produced by power generation. This is the opposite result compared to the Ru catalysts. For comparison, the α of PEFC using Pt catalyst is shown in Table 1 [26]. In PEFC with a Pt catalyst, the D isotope was also preferentially oxidized as experienced with the AFC_{Pt} results presented here.

The isotope separation was inversed between Ru and Pt [32]. The HOR consists of three elementary steps. When an alkali aqueous electrolyte is used, the steps are expressed by following;



Where L is symbol of H or D, and L_{ad} is a hydrogen atom adsorbed on the catalyst.

For Ru catalyst, the Tafel-Volmer combination is the main reaction path of hydrogen oxidation. The Volmer step with the charge transfer reaction is the rate determining [10, 33]. From the impedance results (Fig. 3), there is a significant difference in charge transfer resistance between H and D. Moreover, the desorption of hydrogen adatoms presumably contributes to the reaction rate of the Volmer step. The binding energy is -2.72 eV for H-Ru and -2.77 eV for D-Ru, respectively [34]. Since the desorption force of D-Ru is larger than that of H-Ru, D is not easily detached from the Ru catalyst surface. That is, the slow rate of D_{ad} detachment causes the less D_2 gas consumption, resulting in D enrichment in the gas exhausted from AFC_{Ru} . As another possibility, Ru adsorbs water molecules and hydronium ions more easily than Pt. If the adsorption tendency could be influenced by the mass number, the gas adsorption side at Eq. (3) would be blocked and the D_2 reaction rate might be reduced.

In the Pt catalyst case, Tafel-Volmer at low overpotential and Heyrovsky-Volmer at high overpotential occurs on the Pt catalyst [33]. Both Heyrovsky and Volmer steps, which accompany a charge transfer, hardly contribute to the isotope separation as illustrated by the Nyquist plots of H and D which are almost identical (Fig. 3). Therefore, the Tafel step may be important. The binding energy is -2.62 eV for H-Pt and -2.66 eV for D-Pt, respectively [34]. The reaction of D_2 with higher binding energy occurs preferentially at the Tafel step, where a gas molecule is dissociated and adsorbed on Pt atoms. Therefore, unlike the AFC_{Ru} results, more D_2 gas is consumed during AFC_{Pt} power generation.

4. Conclusions

This research demonstrates D separation using AFC_{Ru} and AFC_{Pt}. When the AFC_{Ru} is operated, the cell voltage when using D₂ as fuel is lower than that when using H₂. The impedance measurement indicates the larger charge transfer resistance for D compared to H, resulting in the slow oxidation reaction of D₂. The power performance of AFC_{Pt} is better than that of AFC_{Ru} and is not dependent on the gas species. The isotope separation was investigated when AFCs were operated at 0.5 A with using 1.0 at% D₂ mixture gas. The α value of AFC_{Ru} is 0.85 and D is enriched as product water, while α of AFC_{Pt} is 1.08. This inverse phenomenon, depending on the catalyst might be related to the differences in adsorption energy between the hydrogen atom and the catalyst surface for the two isotopes. The presented results demonstrate that the D concentration could be controlled by selecting proper catalysts. This will be meaningful knowledge for the isotope separation processes in the field of fusion reactor and material development [35-37].

Acknowledgments

The authors are grateful for financial support from the Ministry of Education, Culture, Sports, Science and Technology (Project No. 17H03528).

Figure Captions

Figure 1

Schematic illustration of isotope separation measurement using an alkaline fuel cell.

Figure 2

Current / cell voltage plots of alkaline fuel cell with Ru (●: AFC_{Ru}) and Pt (○: AFC_{Pt}) anode catalyst when supplying H₂ (red) and D₂ (blue) gas. (Temperature, 323 K; Cathode catalyst, Pt).

Figure 3

Current / potential plots of cathode (■) and anode (□) at AFC_{Ru} when supplying H₂ (red) and D₂ (blue) gas. (Temperature, 323 K; Cathode catalyst, Pt).

Figure 4

Complex plane plots for AFC_{Ru} (●) and AFC_{Pt} (○) when supplying H₂ (red) and D₂ (blue) gas. (Temperature, 323 K; Cathode catalyst, Pt).

Figure 5

Transient behavior of ionization currents of mass components (i_{H_2} ; red, i_{HD} ; blue, i_{D_2} ; green) during AFC_{Ru} operation at 0.5 A with 1.0 at% D₂ mixture gas.

Table 1 Separation factor, α , of AFC_{Ru}, AFC_{Pt} and PEMFC.

References

1. G. F. Mclean, T. Niet, S. Prince-Richard, N. Djilali, An assessment of alkaline fuel cell technology, *Int. J. Hydrog. Energy* 2002;27:507-526.
2. K. Kordesch, V. Hacker, J. Gsellmann, M. Cifrain, G. Faleschini, P. Enzinger, R. Fankhauser, M. Ortner, M. Muhr, R. R. Aronson, Alkaline fuel cells applications, *J. Power Sources* 2000;86:162-165.
3. Z. F. Pan, R. Chen, L. An, Y. S. Li, Alkaline anion exchange membrane fuel cells for cogeneration of electricity and valuable chemicals, *J. Power Sources* 2017;365:430-445.
4. A. Verma, S. Basu, Experimental evaluation and mathematical modeling of a direct alkaline fuel cell, *J. Power Sources* 2007;168:200-210.
5. E. Gülzow, M. Schulze U. Gerke, Bipolar concept for alkaline fuel cells, *J. Power Sources* 2006;156:1-7.
6. J. Durst, A. Siebel, C. Simon, F. Hasché, J. Herranz, H. A. Gasteiger, New insights into the electrochemical hydrogen oxidation and evolution reaction mechanism, *Energy Environ. Sci.* 2014;7:2255-2260.
7. W. Sheng, H. A. Gasteiger, Y. Shao-Horn, Hydrogen Oxidation and Evolution Reaction Kinetics on Platinum: Acid vs Alkaline Electrolytes, *J. Electrochem. Soc.* 2010;157:B1529-B1536.
8. K. J. P. Schouten, M. J. T. C. Van Der Niet, M. T. M. Koper, Impedance spectroscopy of H and OH adsorption on stepped single-crystal platinum electrodes in alkaline and acidic media, *Phys. Chem. Chem. Phys.* 2010;12:15217-15224.
9. X. P. Qin, L. L. Zhang, G. L. Xu, S. Q. Zhu, Q. Wang, M. Gu, X. Y. Zhang, C. J. Sun, P. B. Balbuena, K. Amine, M. H. Shao, The Role of Ru in Improving the Activity of Pd toward Hydrogen Evolution and Oxidation Reactions in Alkaline Solutions, *ACS Catal.* 2019;9:9614-9621.
10. J. K. Li, S. Ghoshal, M.K. Bates, T. E. Miller, V. Davies, E. Stavitski, K. Attenkofer, S. Mukerjee, Z. F. Ma, Q. Y. Jia, Experimental Proof of the Bifunctional Mechanism for the Hydrogen Oxidation in Alkaline Media, *Angew. Chemie - Int. Ed.* 2017;56:15594-15598.
11. R. Tanii, R. Ogawa, H. Matsushima, M. Ueda, Measurement of deuterium isotope separation by polymer electrolyte fuel cell stack, *Int. J. Hydrog. Energy* 2019;44:1851-1856.
12. A. Pozio, S. Tosti, Isotope effects H/D in a PEFC with Pt-Ru/anode at low and high current density, *Int. J. Hydrog. Energy* 2019;44:7544-7554.
13. S. Yanase, T. Oi, Observation of H/D isotope effects on polymer electrolyte membrane fuel cell operations, *J. Nucl. Sci. Technol.* 2013;50:808-812.
14. D. Bessarabov, H. Wang, H. Li, N. Zhao ed., *PEM Electrolysis for Hydrogen Production*, CRC Press 2016:361.
15. E. W. Washburn, H. C. Urey, Concentration of the H-2 isotope of hydrogen by the fractional

- electrolysis of water *Proc. Natl. Acad. Sci. United States Am.* 1932;18:496-498.
16. B. Topley, H. Eyring, The Separation of the Hydrogen Isotopes by Electrolysis, *J. Chem. Phys.* 1934;2:217-230.
 17. R. Bhattacharyya, K. Bhanja, S. Mohan, Simulation studies of the characteristics of a cryogenic distillation column for hydrogen isotope separation, *Int. J. Hydrog. Energy* 2016;41:5003-5018.
 18. S. Fukada, Tritium Isotope Separation by Water Distillation Column Packed with Silica-gel Beads, *J. Nucl. Sci. Technol.* 2004;41:619-623.
 19. T. Sugiyama, Y. Asakura, T. Uda, Y. Abe, T. Shiozaki, Y. Enokida, I. Yamamoto, Preliminary Experiments on Hydrogen Isotope Separation by Water-Hydrogen Chemical Exchange under Reduced Pressure, *J. Nucl. Sci. Technol.* 2004;41:696-701.
 20. K. Harada, R. Tanii, H. Matsushima, M. Ueda, K. Sato, T. Haneda, Effects of water transport on deuterium isotope separation during polymer electrolyte membrane water electrolysis, *Int. J. Hydrog. Energy* 2020;45:31389-31395.
 21. D. Greenway, E. B. Fox, A. A. Ekechukwu, Proton exchange membrane (PEM) electrolyzer operation under anode liquid and cathode vapor feed configurations, *Int. J. Hydrog. Energy* 2009;34:6603-6608.
 22. D. L. Stojić, T. D. Grozdić, M. P. Marčeta Kaninski, A. D. Maksić, N. D. Simić, Intermetallics as advanced cathode materials in hydrogen production via electrolysis, *Int. J. Hydrog. Energy* 2006;31:841-846.
 23. F. Huang, C. Meng, Hydrophobic platinum–polytetrafluoroethylene catalyst for hydrogen isotope separation, *Int. J. Hydrog. Energy* 2010;35:6108-6112.
 24. H. Matsushima, T. Nohira, T. Kitabata, Y. Ito, A novel deuterium separation system by the combination of water electrolysis and fuel cell, *Energy* 2005;30:2413-2423.
 25. R. Ogawa, R. Tanii, R. Dawson, H. Matsushima, M. Ueda, Deuterium isotope separation by combined electrolysis fuel cell, *Energy* 2018;149:98-104.
 26. S. Shibuya, H. Matsushima, M. Ueda, Study of Deuterium Isotope Separation by PEFC, *J. Electrochem. Soc.* 2016;163:F704-F707.
 27. R. Ogawa, H. Matsushima, M. Ueda, Hydrogen isotope separation with an alkaline membrane fuel cell, *Electrochem. Commun.* 2016;70:5-7.
 28. T. Y. George, T. Asset, A. Avid, P. Atanassov, I. V. Zenyuk, Kinetic Isotope Effect as a Tool To Investigate the Oxygen Reduction Reaction on Pt-based Electrocatalysts - Part I: High-loading Pt/C and Pt Extended Surface, *ChemPhysChem.* 2020;21:469-475.
 29. D. Malko, A. Kucernak, Kinetic isotope effect in the oxygen reduction reaction (ORR) over Fe-N/C catalysts under acidic and alkaline conditions, *Electrochem. Commun.* 2017;83:67-71.
 30. M. Beltowska-Brzezinska, T. Luczak, J. Stelmach, R. Holze, The electrooxidation mechanism

of formic acid on platinum and on lead ad-atoms modified platinum studied with the kinetic isotope effect, *J. Power Sources* 2014;251:30-37.

31. W. Phompan, N. Hansupalak, Improvement of proton-exchange membrane fuel cell performance using platinum-loaded carbon black entrapped in crosslinked chitosan, *J. Power Sources* 2011;196:147-152.
32. E. C. M. Tse, T. T. H. Hoang, J. A. Varnell, A. A. Gewirth, Observation of an Inverse Kinetic Isotope Effect in Oxygen Evolution Electrochemistry, *ACS Catal.* 2016;6:5706-5714.
33. K. Elbert, J. Hu, Z. Ma, Y. Zhang, G. Y. Chen, W. An, P. Liu, H. S. Isaacs, R. R. Adzic, J. X. Wang, Elucidating Hydrogen Oxidation/Evolution Kinetics in Base and Acid by Enhanced Activities at the Optimized Pt Shell Thickness on the Ru Core, *ACS Catal* 2015;5:6764-6772.
34. Y. Bai, B. W. J. Chen, G. Peng, M. Mavrikakis, Density functional theory study of thermodynamic and kinetic isotope effects of H-2/D-2 dissociative adsorption on transition metals, *Catal. Sci. Technol.* 2018;8:3321-3335.
35. M. Y. Yang, J. B. Zhou, L. P. Gao, The purification of hydrogen isotopes expelled from nuclear fusion reactors by a combined process, *Int. J. Hydrog. Energy* 2020;45:13596-13600.
36. W. J. Byeon, S. K. Lee, S. J. Noh, Transport of hydrogen and deuterium in 316LN stainless steel over a wide temperature range for nuclear hydrogen and nuclear fusion applications, *Int. J. Hydrog. Energy* 2020;45:8827-8832.
37. M. Glugla, R. Lasser, L. Dorr, D. K. Murdoch, R. Haange, H. Yoshida, The inner deuterium/tritium fuel cycle of ITER, *Fusion Eng. Des.* 2003;69:39-43.

Table 1 Separation factor, α , of AFC_{Ru}, AFC_{Pt} and PEMFC.

Type of FC	α
AFC _{Ru}	0.85
AFC _{Pt}	1.08
PEMFC	2.0~3.0

Figure 1

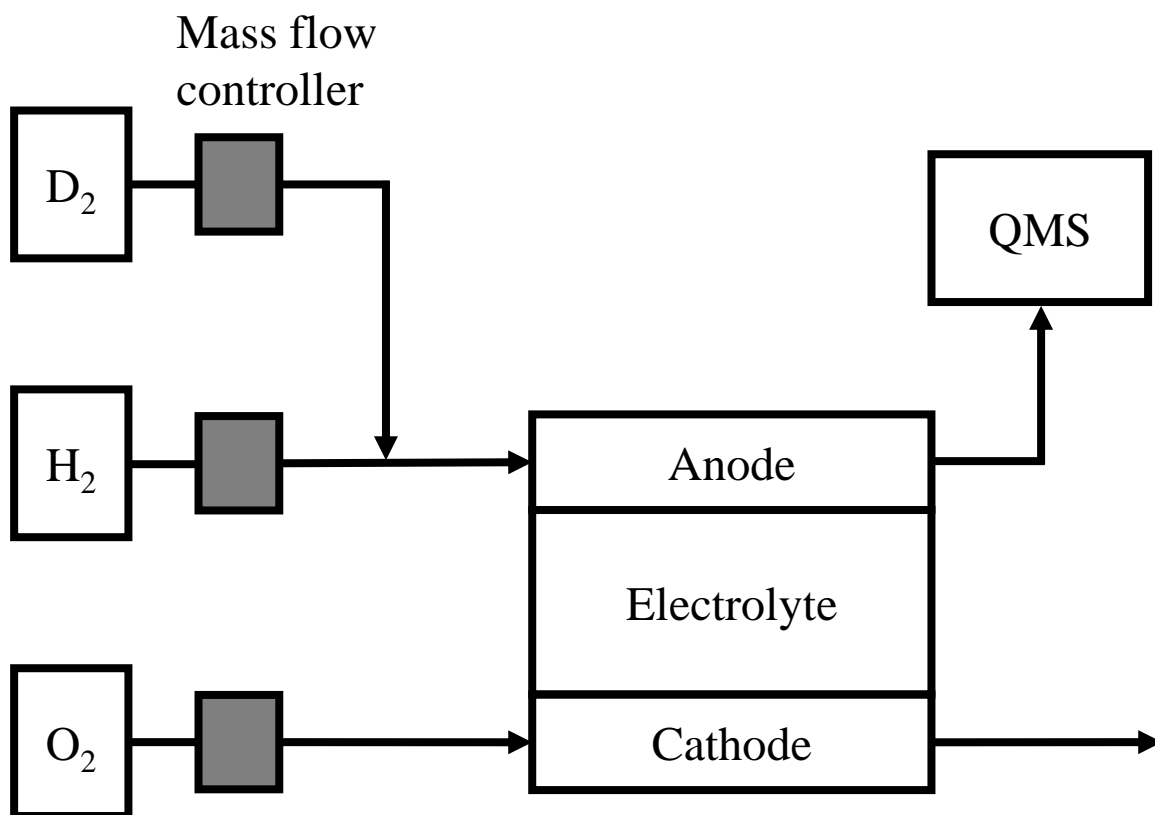


Fig. 1

Figure 2

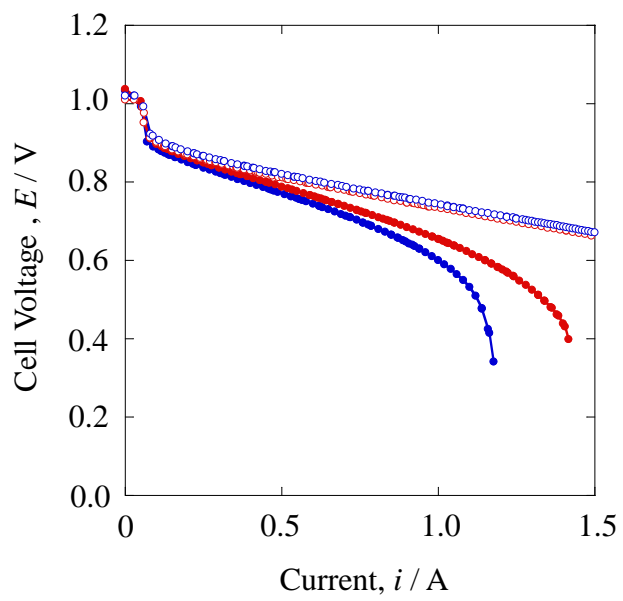


Fig. 2

Figure 3

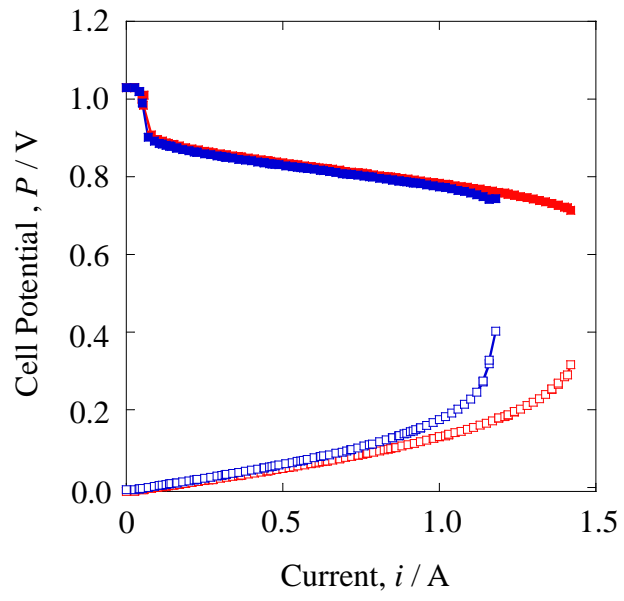


Fig. 3

Figure 4

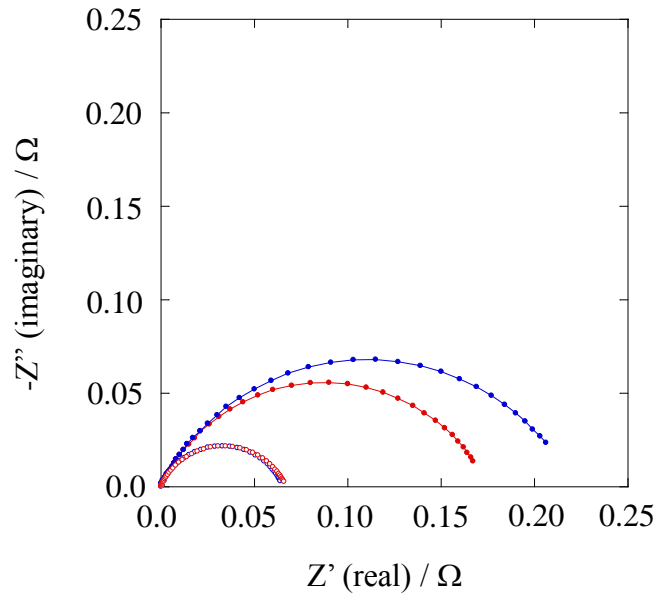


Fig. 4

Figure 5

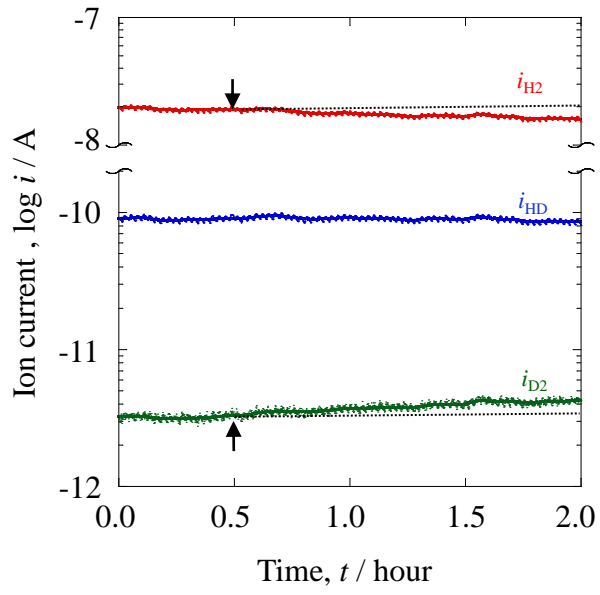


Fig. 5

Declaration of interests

The authors declare that they have no known competing financial interests or personal relationships that could have appeared to influence the work reported in this paper.

The authors declare the following financial interests/personal relationships which may be considered as potential competing interests: